The Distribution of Helium 3 in the Deep Western and Southern Indian Ocean

Daniel Jamous, Laurent Mémery, Chantal Andrié, Philippe Jean-Baptiste, Liliane Merlivat

JOURNAL OF GEOPHYSICAL RESEARCH, VOL. 97, NO. C2, PAGES 2243–2250, FEBRUARY 15, 1992

The Distribution of Helium 3 in the Deep Western and Southern Indian Ocean

DANIEL JAMOUS,[1] LAURENT MÉMERY,[2] CHANTAL ANDRIÉ,[2] PHILIPPE JEAN-BAPTISTE,[1] AND LILIANE MERLIVAT[2]

Almost a decade after the Geochemical Ocean Sections Study Indian Expedition, the new deep ^{3}He data from the INDIGO program give a further insight into the distribution of this tracer in the Indian Ocean. This distribution exhibits some major features related on one hand to a hydrothermal ^{3}He input in the Gulf of Aden and on the Mid–Indian Ocean Ridge, and on the other to the origin of the water masses and to the characteristics of the deep circulation. The main pattern is a significant north-south ^{3}He gradient, with deep waters of the southern ocean showing δ^3He values around 8–9% due to the influence of the Atlantic deep waters poor in ^{3}He and relatively high values in the northern and central regions (15% to 18% between 2000 m and 3000 m depth) originating from the hydrothermal activity. In the easternmost part of the basin, the ^{3}He values exhibit a significant increase at shallower depths (around 1000 m) probably due to the Pacific water flow through the Indonesian sills, whereas the data in the Indian sector of the Antarctic ocean show a maximum of the order of 10%, south of the Polar Front, interpreted as showing the presence of the Pacific deep waters in the Antarctic Circumpolar Current. These different aspects are summarized by mapping the horizontal distribution of the δ^3He maxima all over the Indian basin. This map points out some characteristics of the deep circulation but also stresses the need for further measurements in order to clarify the description of this tracer in several key areas.

INTRODUCTION

There are two main sources of ^{3}He in the ocean. The first of these is production by the β decay of anthropogenic tritium in the mixed layer and in the thermocline. In the deep ocean the ^{3}He distribution is controlled by the primordial hydrothermal input and the deep circulation [*Clarke et al.*, 1969; *Craig and Lupton*, 1981]. This distribution is assumed to be at steady state, which is reasonable when comparing the deep ocean renewal time to the time scale of the processes controlling the mantle degassing at oceanic ridges. The present study deals with this deep, steady distribution.

In the last decade, ^{3}He injection sites associated with hydrothermal activity have been found at many different places on mid-ocean ridges. On a global scale, the Geochemical Ocean Sections Study (GEOSECS) ^{3}He survey carried out in the 1970s is the most comprehensive data set available so far. This pioneer work made possible a first estimation of the distribution of ^{3}He in the different oceans. The deep Pacific Ocean is the most enriched in ^{3}He (with a mean δ^3He value below the thermocline of around 17%) compared with the Indian Ocean ($\langle\delta\rangle \sim 10\%$), the southern ocean ($\langle\delta\rangle \sim 7\%$) and the Atlantic ($\langle\delta\rangle \sim 2\%$). The reason for such a strong contrast lies primarily in the varying strength of the hydrothermal input, as well as in the difference in ventilation rate of the deep basins [*Jean-Baptiste*, 1992]. More specifically, the GEOSECS Indian Ocean data have already shown deep meridional gradients with higher values in the northern part of the basin [*Lupton and Craig*, 1980; *Ostlund et al.*, 1987].

New ^{3}He measurements have been obtained in the western and southern Indian Ocean from the French program INDIGO (1985–1987). The main scientific purpose was to sample the western basin of the Indian Ocean, a decade after GEOSECS, in order to obtain an updated distribution of transient tracers and to evaluate the invasion and transport of anthropogenic carbon in this area. Measurements of several geochemical tracers among them ^{3}He, were carried out. Although the sampling strategy was focused on the penetration of transient tritium/helium 3 in the thermocline, 500 deep samples were collected as well. This complementary data set enables us to investigate further the deep ^{3}He distribution in the Indian Ocean. Locations of the stations are shown in Figure 1*a* along with the ^{3}He sections that are discussed later in the text (Figure 1*b*).

Also included in our analysis are a few ^{3}He measurements carried out on the Indian Ocean ridges (see Figure 1) and available in the literature: MD-34 (*Marion Dufresne* cruise 34) data obtained by us on the Southwest Indian Ocean Ridge in 1983, GEODYN (P. Jean-Baptiste et al., Hydrothermal helium-3 and manganese plumes at 19°29′ south on the Central Indian Ridge, submitted to *Geophysical Research Letters*, 1991, hereinafter Jean-Baptiste et al., 1991) and GEMINO-1 data [*Herzig and Pluger*, 1988] from the Central Indian Ocean Ridge, and OCEAT ^{3}He measurements [*Jean-Baptiste et al.*, 1990] from the Gulf of Aden.

In the following, some experimental details of the INDIGO measurements run at Saclay, France, are discussed, and an intercomparison of both the GEOSECS and INDIGO sets of data is carried out. The data are then presented in two separate sections: the Antarctic sector and the western and central Indian Ocean.

All the INDIGO rosette data, including ^{3}He are available from the INDIGO cruise reports [*Poisson et al.*, 1988, 1989, 1990].

EXPERIMENTAL METHOD AND DATA ANALYSIS

Seawater samples were collected by means of a rosette system fitted with 10-L Niskin bottles and conductivity-temperature-depth (CTD) sensors. Helium samples were

[1]Laboratoire de Géochimie Isotopique, Saclay, Gif-Sur-Yvette, France.
[2]Laboratoire d'Océanographie Dynamique et de Climatologie, Paris.

Paper number 91JC02062.
0148-0227/92/91JC-02062$05.00

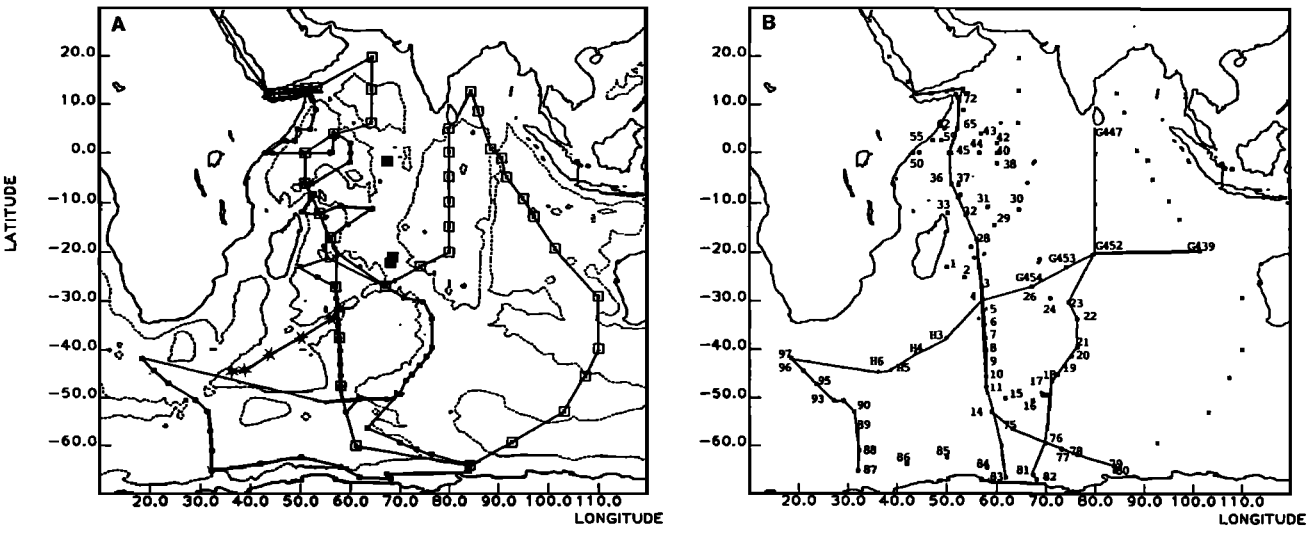

Fig. 1. (*a*) Indian Ocean map with its 4000-m isobath, showing the main cruise tracks and station locations: solid dots, INDIGO; open squares, GEOSECS; stars, MD-34 (Southwest Indian Ocean Ridge) and OCEAT (Gulf of Aden); solid squares, GEMINO and GEODYN data (Mid-Indian Ocean Ridge). (*b*) Location of the ^{3}He sections discussed in text.

sealed in 40-cm^3 copper tubes and returned to the laboratory for determination of the isotopic composition of dissolved helium. The procedure for extracting and analyzing the helium isotopes is basically the one described by *Clarke et al.* [1976]. The overall uncertainty in the ^{3}He excess (δ^3He (percent) = $(R/R_a - 1) \times 100$, where R is the isotopic ratio of the sample and R_a is the atmospheric ratio) is of the order of ±0.4% [*Jean-Baptiste et al.*, 1988].

Neon Interference

As no neon trap was used with our mass spectrometer, we investigated the neon interference with our ^{3}He measurements by running a series of our standard air aliquot (the size of which corresponds to the amount of helium present in 40 cm^3 of seawater) with an added amount of neon equal to the difference between the amount of neon in this air aliquot and the amount of neon dissolved in a 40-cm^3 seawater sample.

This was done using a Ne/Ar mixture (18.7 ppm Ne) kept in a tank equipped with a 0.079-cm^3 aliquot and fitted on the introduction line of the mass spectrometer.

The comparison between the two series of measurements (10 measurements of our standard alone and 10 measurements of standard plus additional Ne) leads to a positive offset of δ = +0.3% caused by neon. Although this value is within our experimental uncertainty, all our δ^3He data have been corrected by subtracting 0.3% to take into account the neon effect.

INDIGO-GEOSECS Intercomparison

In order to use both sets of data together when needed, because the magnitudes of the δ^3He horizontal variations are of the order of a few percent most of the time, it is necessary to look carefully at the comparison between the two data sets. This was done from the GEOSECS stations that were reoccupied during INDIGO. The result is shown in Figure 2. Data from the MEROU cruise [*Andrié and Merlivat*, 1989] in the Red Sea and from the Gulf of Aden [*Jean-Baptiste et al.*, 1990], obtained on the same mass spectrometer, have also been included to extend the plot over a wider range of δ^3He values. Although these data are more scattered, possibly because of the much larger spatial ^{3}He gradient in this area, they offer a better determination of the slope of the correlation. Only near-surface data and data below 1000 m are considered on account of the significant transient tritiumgenic ^{3}He component likely to occur at intermediate depths.

Taking into account the error bars on each individual value (±0.4% for INDIGO, ±1% for GEOSECS and ±2% for both labs in the Red Sea and the Gulf of Aden), we obtain a regression line

$$(\delta^3\mathrm{He})_{\mathrm{INDIGO}} = (\delta^3\mathrm{He})_{\mathrm{GEOSECS}} \times (1.05 \pm 0.03) + (0.4 \pm 0.4)\%$$

corresponding to the shaded area of Figure 2.

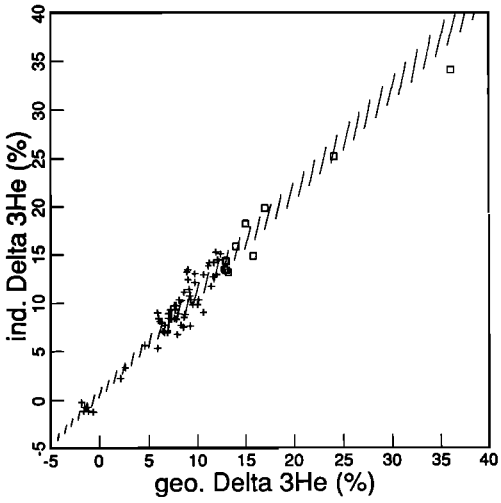

Fig. 2. Plot of $\delta^3\mathrm{He}_{\mathrm{INDIGO}}$ versus $\delta^3\mathrm{He}_{\mathrm{GEOSECS}}$ for the GEOSECS stations reoccupied during INDIGO (crosses). GEOSECS data are interpolated at the depths of the INDIGO samples. Open squares correspond to data from the Red Sea and Gulf of Aden. Only near-surface data and data below 1000 m are considered (see text).

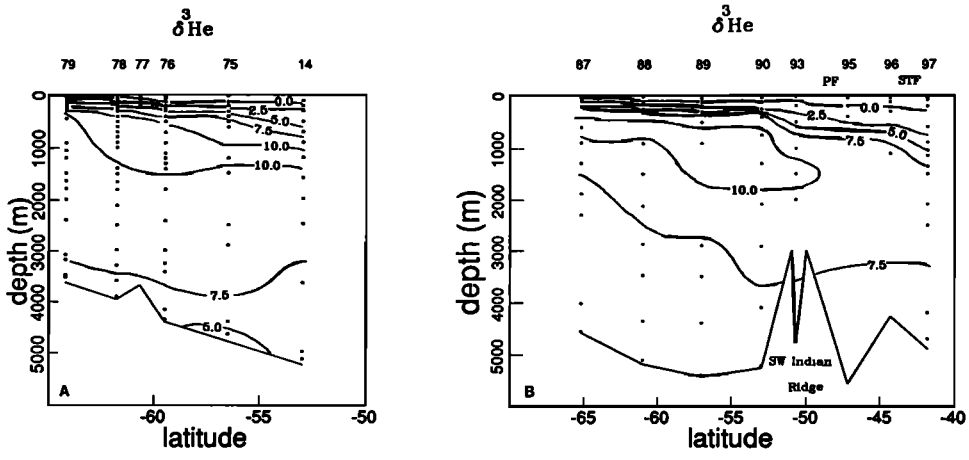

Fig. 3. Two INDIGO δ^3He sections across the southern ocean (see Figure 1*b* for section locations). (*a*) Stations 79–14. (*b*) Stations 87–97.

This plot leads us to conclude that there is no statiscally meaningful bias between the two sets of data in the range of interest (0 to 15%). Therefore we consider in the following that they can be merged for a common use without any adjustment.

Results and Discussion

Antarctic Sector

The main pattern that emerges from the ^{3}He distribution in the southern ocean is a 10% δ^3He core centered around 1000 m depth, very clearly seen on the two INDIGO ^{3}He sections and across the circumpolar ocean shown in Figure 3. This feature extends from the southernmost stations close to the Antarctic continental shelf to approximately the latitude of the Polar front. Further north, all the δ^3He values fall below 10%, indicating the influence of North Atlantic Deep Water (NADW) poor in ^{3}He and whose core lies just south of the Cape of Good Hope [*Jacobs and Georgi*, 1977]. The δ^3He maximum occurs approximately at the depth of the oxygen minimum that marks the top of the Circumpolar Deep Water (CDW). This water mass is characterized by a deep salinity maximum found below the oxygen minimum and is brought eastward by the Antarctic Circumpolar Current (ACC) [*Wyrtki*, 1973]. Because of the upwelling occurring at the level of the Antarctic divergence (~65°S), all the extreme values of the properties rise south of the Polar front. At depth, the δ^3He values decrease down to 5–6% in the Antarctic Bottom Water owing to the more recent ventilation of this water mass.

These main characteristics are easily observed on the selection of profiles shown in Figure 4: all profiles except station 97 are located south of the Polar front. In this region, the first 100 m of the water column are characterized by a very cold layer, close to the freezing point (Winter Water), above which is found, during summer, a somewhat less cold surface water (Summer Surface Water) [*Gamberoni et al.*, 1990]. Just below these shallow waters, the Circumpolar Deep Water is very well identified from its enhanced temperature and salinity. These hydrologic features are responsible for the sharp subsurface increase of the δ^3He apparent in all profiles, which rapidly reaches values around 10% typical of the CDW.

Station 97, situated north of the subtropical convergence, displays quite a different picture, with a strong erosion of the δ^3He maximum that was present at intermediate depths on the other profiles, due to the intrusion of Atlantic waters.

Coming back to the ^{3}He core described above, it is interesting to note that a similar pattern is also visible in the western Pacific and western Atlantic GEOSECS sections and then appears to be a permanent feature all around the circumpolar ocean. This ^{3}He maximum could have a local origin due to some hypothetical hydrothermal activity related to the southern ocean ridges. Indeed, some indications of ^{3}He primordial injection were reported by *Schlosser et al.* [1988] in the Bransfield Strait.

Although this explanation cannot be completely ruled out, we favor a second possibility, which is an origin in the eastern Pacific where high ^{3}He concentrations are well established [*Lupton and Craig*, 1981]. Unfortunately, the eastern Pacific GEOSECS ^{3}He section does not extend far enough south to give direct evidence of this fact. This possibility, already suggested by *Callahan* [1972] and *Jenkins and Clarke* [1976], is supported by the correlation between the ^{3}He maximum and the oxygen minimum. Strikingly, the lowest oxygen concentrations in the region are found precisely in the southeastern Pacific with a core of low-oxygen water (3.3 mL/L) around 1500 m depth close to the South American coast [*Gordon et al.*, 1982]. This low-oxygen water mass can be traced in the Drake Passage showing a layer of O_2-depleted waters at the same depth along the South American coast, which rises southward up to 500 m depth when approaching the Antarctic continental slope (Figure 5).

This ^{3}He core also corresponds to a minimum in the chlorofluorocarbon CFC-11 that is well defined in the CFC-11 *Ajax* section by *Warner* [1988], meaning that this water mass is older than the surrounding waters. These different indications are consistent with ^{3}He-rich, O_2/CFC-depleted Pacific waters penetrating the southern ocean in the vicinity of the Drake Passage.

Furthermore, this inverse correlation between the oxygen and ^{3}He distributions is a broad feature of the southern ocean (Figure 6) which reflects the fact that both tracers' distributions here are being primarily governed by ventilation processes. This is clearly seen at the southernmost

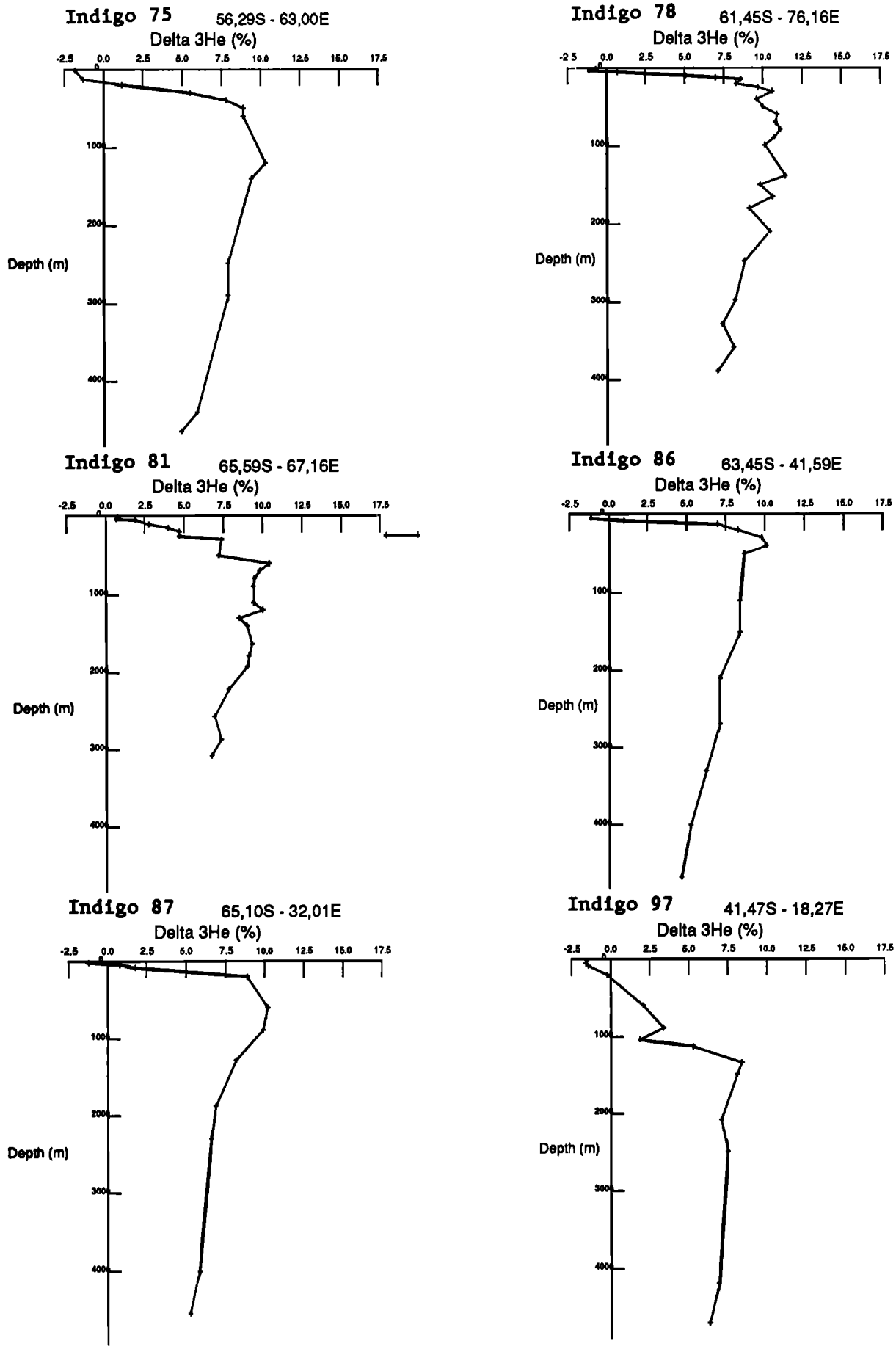

Fig. 4. Display of some ^{3}He profiles from the Indian sector of the southern ocean.

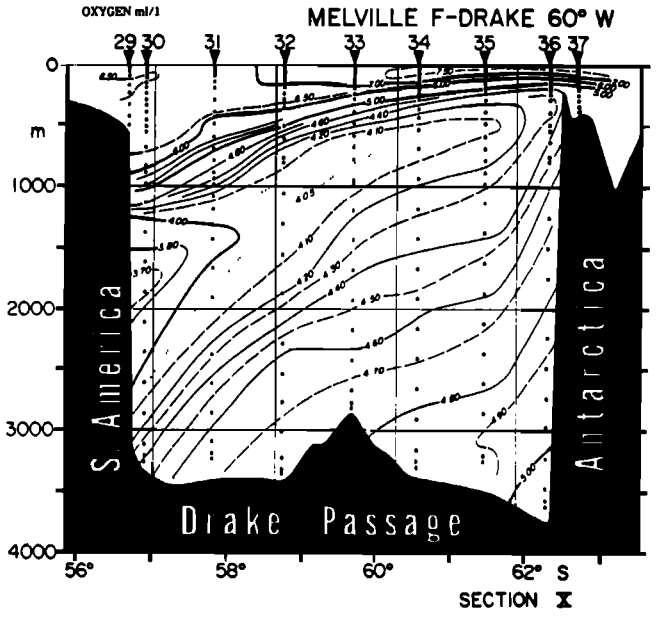

Fig. 5. Oxygen section in the Drake Passage from the *Southern Ocean Atlas* [*Gordon et al.*, 1982].

stations INDIGO 80, 81, and especially 82 and 83 located on the continental slope (Figure 7). There, ^{3}He and O_2 profiles agree in pointing out the formation of dense water along the continental shelf showing higher O_2 as well as lower δ^3He values at the bottom of both stations.

Western and Central Indian Ocean

The ^{3}He distribution in the western and central Indian Ocean is characterized by several distinct features apparent on the three ^{3}He sections displayed in Figures 8*a*, 8*b* and Figure 9.

The Gulf of Aden component. The first prominent pattern (Figure 8*a*) is the deep north-south gradient already observed in the GEOSECS data [*Ostlund et al.*, 1987]. South of 40°S, the δ^3He values are typically less than 10% with an upward slope of the isolines. From the Gulf of Aden to the equator, a broad area of high values (15%) is present all along the westernmost track at depths between 1500 m and 3500 m. With regard to other properties' extremes, the deep δ^3He maximum is close to the deep salinity maximum but above the deep silica maximum present in the Indian Ocean at depths of about 3000–4000 m, originating at the bottom of Arabian sea and the Bay of Bengal from siliceous sediments [*Edmond et al.*, 1979].

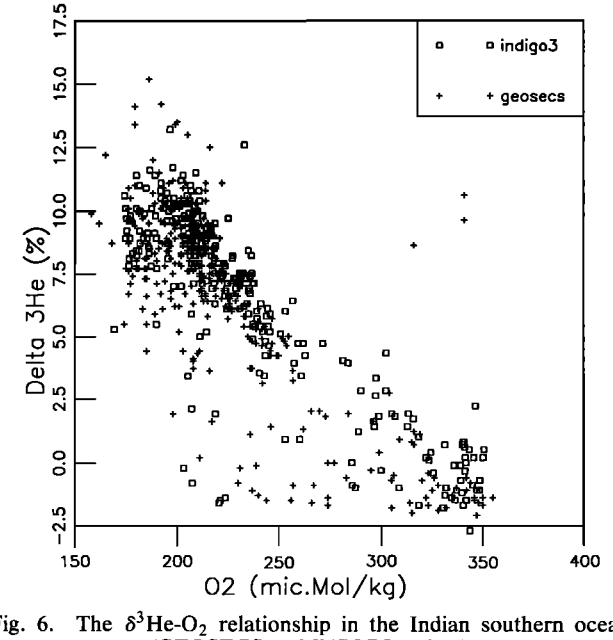

Fig. 6. The δ^3He-O_2 relationship in the Indian southern ocean (GEOSECS and INDIGO 3 data)

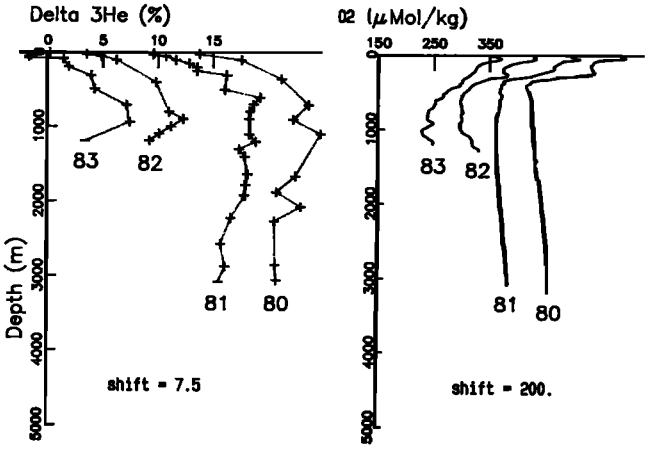

Fig. 7. Profiles of δ^3He and O_2 on the Antarctic continental slope (INDIGO 3 stations 80 through 83)

These ^{3}He enriched waters come from the Gulf of Aden where a significant ^{3}He primordial input (with ^{3}He excesses of up to 49%) has been reported [*Jean-Baptiste et al.*, 1990]. The flow of deep waters from the Gulf of Aden is poorly documented. Recent studies indicate a southwestward deep flow in the Somali basin. Near 3°N, 53°E, *Fieux et al.* [1986] report anticlockwise geostrophic boundary currents below a zero-surface reference of 2000 dbar in April 1985. Moreover, the distribution of the INDIGO 2 salinity data (April 1986) on the surface of a potential temperature of 1.8°C (mean depth, 2600 m) suggests a southwestward penetration of saline waters along the Somali coast [*Schott et al.*, 1989]. The large ^{3}He excesses that we observe are consistent with this southwestward flow. This implies that the Gulf of Aden deep waters turn south when passing the island of Socotra, where there are passages as deep as 3000 m.

This possible deep circulation scheme is apparent in Figure 10, which displays the horizontal distribution of the deep ^{3}He maxima over the whole Indian basin. At the equator there are some indications in the data that the high ^{3}He signal is propagating eastward with a series of six stations with ^{3}He maxima over 14% from the African coast (δ^3He = 14.8% at INDIGO station 50) to 80°E (δ^3He = 14.2% at GEOSECS station 448), namely INDIGO 50 (δ% = 14.8); INDIGO 45, 44, and 38 (δ% = 14.4); GEMINO-31WU (δ% = 14.0); and GEOSECS 448 (δ% = 14.2). This zonal pattern could be a deep extension of the intermediate zonal circulation in the equatorial region [*Ponte and Luyten*, 1990; *Jensen*, 1990].

The central Indian primordial ^{3}He input. The central section also displays another ^{3}He feature with increasing values up to 17% in the vicinity of the triple point of the

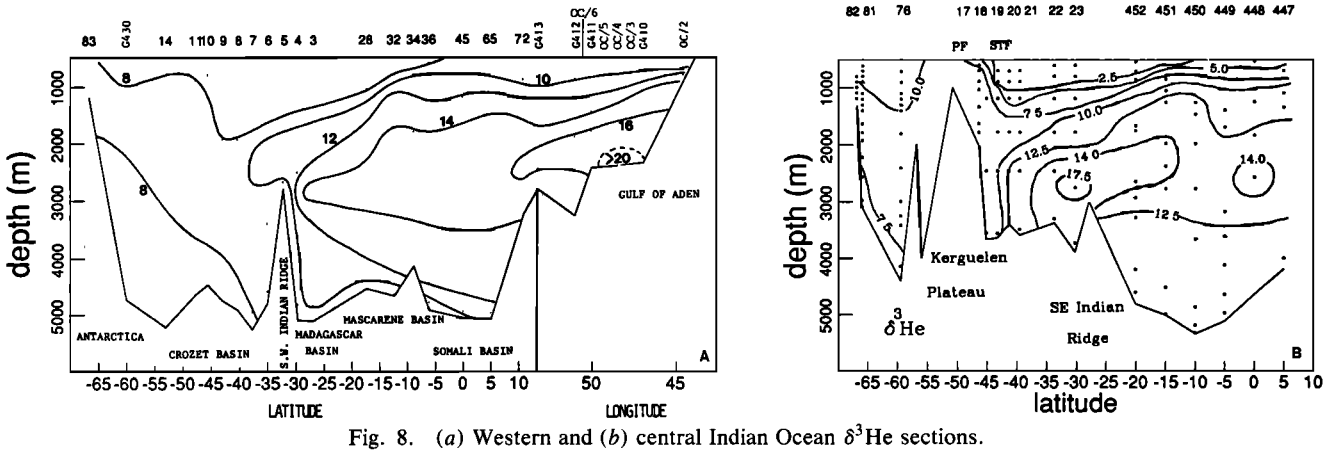

Fig. 8. (*a*) Western and (*b*) central Indian Ocean δ^3He sections.

Indian Ocean ridges (INDIGO station 23). This result is consistent with the German measurements from GEMINO-1 stations 55-WU and 63-WU (21°S, 68°E) showing values up to 18% [*Herzig and Pluger*, 1988]. The possibility that these data suggest some primordial ^{3}He input in this area is fully confirmed by the recent data from the GEODYN cruise (Jean-Baptiste et al., 1991): a ^{3}He plume with values reaching 34%, well correlated with manganese anomalies, has been detected in the same area (19°S, 66°E). This gives the first direct evidence of a significant primordial ^{3}He injection in the region of the Rodriguez Triple Junction (RTJ).

This ^{3}He pattern associated with the Indian ridge and the RTJ is also clearly noticeable on the east-west section from GEOSECS station 439 to INDIGO station 97 (Figure 9).

The Pacific water throughflow. In addition to the hydrothermal signal discussed in the previous section, the δ^3He contours of Figure 9 also display an east-west gradient with increasing ^{3}He values when approaching the Indonesian sector; a value up to 15.4% is recorded at GEOSECS station 439 at 1200 m depth. The fact that this maximum occurs at a shallow depth is consistent with a Pacific Ocean influence through the series of sills of the Indonesian archipelago, the maximum depth of which is around 1000 m (GEBCO, 1984). Also consistent is the δ^3He value of the Pacific Ocean at the entrance of the Indonesian seas, which is of the order of 18% at 1000 m [*Belviso et al.*, 1987]. The first results of the French-Indonesian Java Dynamics Experiment (JADE) in 1989 show westward flows between 0 and 1100 m and much weaker and variable flows at deeper levels [*Fieux et al.*, 1992]. A better image of the ^{3}He distribution east of the GEOSECS track will be obtained from the ^{3}He samples also collected during this cruise.

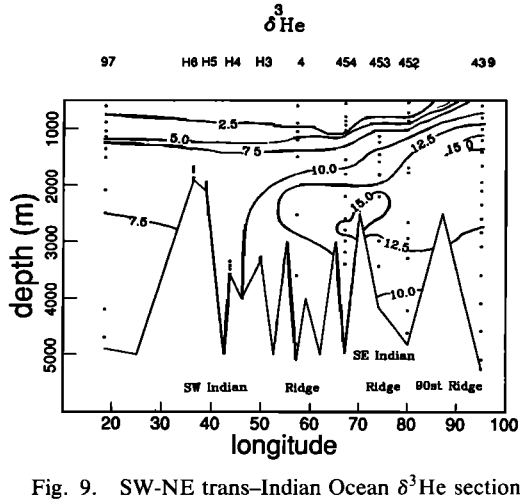

Fig. 9. SW-NE trans-Indian Ocean δ^3He section.

It is difficult to get a global view of the eastern region between this likely intermediate Pacific inflow and the central primordial input owing to the lack of data. Nevertheless, the east-west section of Figure 9 suggests a spreading of the ^{3}He plume toward the east, in connection with a possible deep extension of the anticyclonic circulation of the subtropical gyre [*Wyrtki*, 1973].

The NADW imprint. Along with the ^{3}He features already discussed above, the map of the deep ^{3}He maxima displayed in Figure 10 shows a broad area of low ^{3}He values (δ^3He $\simeq$ 9%) around 40°S. This zonal feature traces the ^{3}He-poor North Atlantic Deep Water, in which enter the Indian basin south of the Cape of Good Hope.

Also noticeable in Figure 10 are some lower δ^3He values extending northward along the African coast, again resulting from the influence of the NADW. The deep circulation of bottom waters in the south of the Somali basin was recently investigated by *Johnson and Warren* [1989]. On a section south of the equator, they observed a deep western boundary current flowing northward along the African continental rise, then turning east near the equator. This eastward extension of waters with a lower ^{3}He content could explain the minimum in the δ^3He values observed in the data between the Gulf of Aden maximum in the northwest and the Rodriguez Triple Junction maximum in the central part of the basin. However the poor spatial resolution of the data in this particular region precludes any definitive answer.

CONCLUSION

This global study of the deep ^{3}He in the Indian Ocean is a first attempt to rationalize the ^{3}He distribution in this ocean from the viewpoint of our current knowledge of both the deep water masses and deep circulation. Thanks to the new data set obtained during the INDIGO cruises in the western part of the basin, some large-scale features, already noticeable in the GEOSECS data, can be described in more detail. The most obvious one is the significant north-south gradient: deep waters carried by the ACC are characterized by low

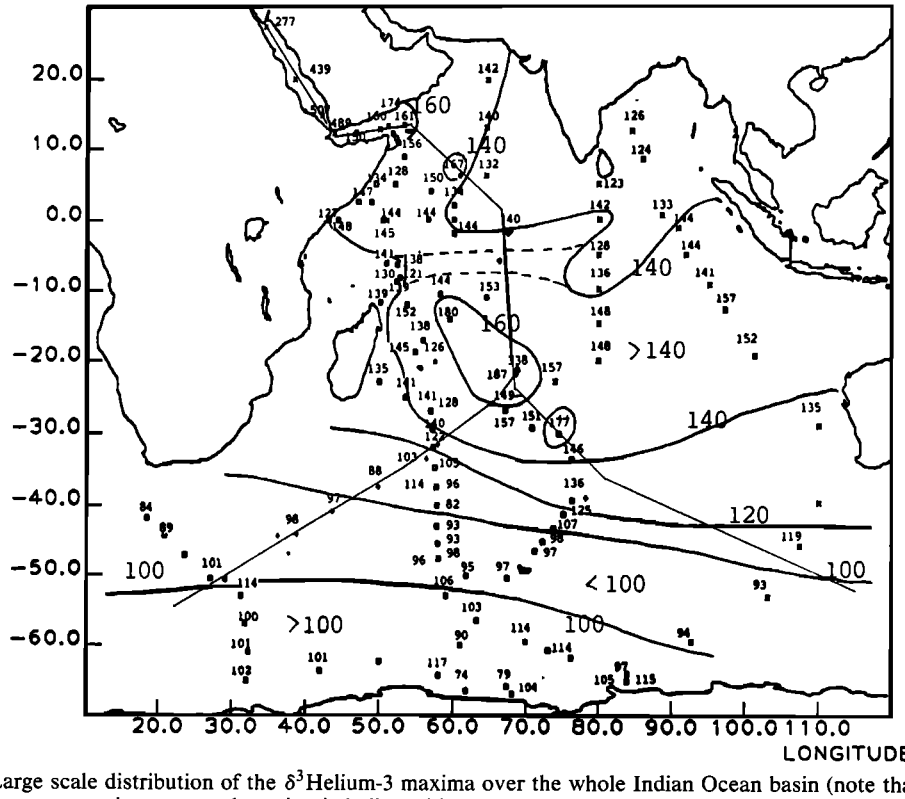

Fig. 10. Large scale distribution of the δ^3Helium-3 maxima over the whole Indian Ocean basin (note that the δ^3He maximum at each station is indicated in permil on the map instead of percent)

δ^3He values (8–9%) reflecting the imprint of the Atlantic waters depleted in ^{3}He, whereas northern waters show δ^3He values above 15% originating from hydrothermal inputs in the Gulf of Aden. South of the Polar front, the signature of the Pacific intermediate waters entering the ACC is documented from two ^{3}He meridional sections.

In the central region, the improvement of the data coverage since the time of GEOSECS allows us to point out a significant hydrothermal component in the vicinity of the Rodriguez Triple Point.

North of 20°S, three main ^{3}He sources are well established: the Gulf of Aden component, the Rodriguez Triple Junction component, and the Pacific throughflow. The ^{3}He gradients are significant all over the basin. This stresses the role of the deep circulation for redistributing this conservative tracer within a basin which is closed in the north.

Except for *Warren*'s [1981, 1982] studies along a section at 18°S and several interesting studies of the deep western boundary currents off the African coast and their equatorial extension [*Fieux et al.*, 1986; *Luyten and Swallow*, 1976; *Luyten et al.*, 1980; *Luyten and Roemmich*, 1982; *Quadfasel and Schott*, 1982; *Schott*, 1986; *Schott et al.*, 1989], little is known as yet of the abyssal circulation in this oceanic basin. This qualitative study shows the potential of ^{3}He as a tracer of this circulation. However, it also exhibits some key regions where more data are necessary to clarify the description of the tracer distribution and hence allow us to go beyond a purely descriptive analysis. One of these regions is the equatorial ocean, with an emphasis on the connection between the Gulf of Aden and the Rodriguez Triple Junction. More information on the deep zonal flows and on the respective influence of the NADW versus Red Sea waters could be obtained from a denser data set. Also necessary is a filling of the gap between the central and the Indonesian/Australian sectors in order to follow the spreading of the ^{3}He sources.

The ^{3}He samples taken during the 1989 JADE experiment, aimed at studying the Pacific throughflow, will increase very significantly the coverage of this key area and its links to the equatorial circulation. Although not yet scheduled, the WOCE (World Ocean Circulation Experiment) Hydrographic Program sections planned in the Indian Ocean will also improve dramatically our knowledge of the deep distribution of this tracer, especially the portion of the meridional sections across the equator as well as the zonal transect around 20°S that intersects the Rodriguez Triple Junction.

Acknowledgments. The authors wish to thank the captain and crew of the R/V *Marion Dufresne*. The present study would not have been possible without the outstanding work of Alain Poisson, in charge of the three INDIGO cruises. We also wish to thank Michelle Fieux, Gilles Reverdin, Nicolas Metzl, and Jean-François Minster for helpful discussions. The INDIGO program was supported by the TAAF (Terres Australes et Antarctiques Françaises). We also acknowledge financial support by the CNRS (Centre National de la Recherche Scientifique) and the CEA (Commissariat à l'Énergie Atomique).

REFERENCES

Andrié, C., and L. Merlivat, Contribution des données isotopiques de deutérium, oxygène-18, hélium-3 et tritium à l'étude de la circulation de la mer Rouge, *Oceanol. Acta*, *12*(3), 165–174, 1989.

Belviso, S., P. Jean-Baptiste, B. C. Nguyen, L. Merlivat, and L. Labeyrie, Deep methane maxima and ^{3}He anomalies across the Pacific entrance to the Celebes basin, *Geochim. Cosmochim. Acta*, *51*, 2673–2680, 1987.

Callahan, J. E., The structure and circulation of deep water in the Antarctic, *Deep Sea Res.*, *19*, 563–575, 1972.

Clarke, W. B., M. A. Beg, and H. Craig, Excess ^{3}He in the sea: Evidence for terrestrial primordial helium, *Earth Planet. Sci. Lett.*, *6*, 213–220, 1969.

Clarke, W. B., W. G. Jenkins, and Z. Top, Determination of tritium by mass spectrometric measurements of ^{3}He, *Int. J. Appl. Radiat. Isot.*, *27*, 515–522, 1976.

Craig, H., and J. E. Lupton, Helium-3 and mantle volatiles in the ocean and the oceanic crust, in *The Sea*, vol. 7, *The Oceanic Lithosphere*, edited by C. Emiliani, pp. 291–428, John Wiley, New York, 1981.

Edmond, J. M., S. S. Jacobs, A. L. Gordon, A. W. Mantyla, and R. F. Weiss, Water column anomalies in dissolved silica over opaline pelagic sediments and the origin of the deep silica maximum, *J. Geophys. Res.*, *84*, 7809–7826, 1979.

Fieux, M., F. Schott, and J. C. Swallow, Deep boundary currents in the western Indian Ocean revisited, *Deep Sea Res.*, *33*, 415–426, 1986.

Fieux, M., C. Andrié, P. Delecluse, A. G. Ilahude, A. Kartavtseff, F. Mantisi, R. Molcard, and J. C. Swallow, Measurements within the Pacific-Indian oceans throughflow region: Preliminary results of the JADE cruise, *Deep Sea Res.*, in press, 1992.

Gamberoni, L., E. Charriaud, and A. Kartavtseff, Les rapports des campagnes à la mer: MD 53/INDIGO 3/SUZAN, *Publ. 87-04*, pp. 141, Mission de Recherche, Terres Australes et Antarctiques Françaises, Paris, 1990.

Gordon, A. L., E. J. Molinelli, and T. N. Baker, *Southern Ocean Atlas*, Columbia University Press, New York, 1982.

Herzig, P. M., and W. L. Pluger, Exploration for hydrothermal activity near the Rodriguez Triple Junction, Indian Ocean, *Can. Mineral.*, *26*, 721–736, 1988.

Jacobs, S. S., and D. Georgi, Observations on the southwest Indian/Antarctic Ocean, in *A Voyage of Discovery*, 70th Anniv. vol., edited by M. Angel and G. Deacon, pp. 43–84, Pergamon, New York, 1977.

Jean-Baptiste, P., The helium-3 distribution in the deep world ocean: Its relation to hydrothermal helium-3 fluxes and to the terrestrial heat budget, in *Isotopes of Noble Gases as Tracers in Environmental Studies, IAEA Processing Panel Ser.*, International Atomic Energy Agency, Vienna, in press, 1992.

Jean-Baptiste, P., C. Andrié, and M. Lelu, Mesure du couple tritiumhélium océanique par spectrométrie de masse, in *Proceedings of the International Symposium on Radioactivity and Oceanography, Radionuclides: A Tool for Oceanography*, edited by J. C. Guary, P. Guegueniat, and R. J. Pentreath, pp. 45–54, Elsevier Science, New York, 1988.

Jean-Baptiste, P., S. Belviso, G. Alaux, N. Mihalopoulos, and B. C. Nguyen, ^{3}He and methane in the Gulf of Aden, *Geochim. Cosmochim. Acta*, *54*, 111–116, 1990.

Jenkins, W. J., and W. B. Clarke, The distribution of ^{3}He in the western Atlantic Ocean, *Deep Sea Res.*, *23*, 481–494, 1976.

Jensen, T. G., Remote forcing of the undercurrents in the Somali current (abstract), *Eos Trans., AGU*, *71*, 1381, 1990.

Johnson, G. C., and B. A. Warren, Circulation of bottom waters in the Somali basin (abstract), *Eos Trans., AGU*, *70*, 1131, 1989.

Lupton, J. E., and H. Craig, Helium-3 in the western Indian Ocean (abstract), *Eos Trans., AGU*, *61*, 987, 1980.

Lupton, J. E., and H. Craig, A major helium-3 source at 15°S on the East Pacific Rise, *Science*, *214*, 13–18, 1981.

Luyten, J. R., and D. H. Roemmich, Equatorial currents at semiannual period in the Indian Ocean, *J. Phys. Oceanogr.*, *12*, 406–413, 1982.

Luyten, J. R., and J. C. Swallow, Equatorial undercurrents, *Deep Sea Res.*, *23*, 999–1001, 1976.

Luyten, J. R., M. Fieux and J. Gonella, Equatorial currents in the western Indian Ocean, *Science*, *209*, 600–603, 1980.

Ostlund, G. H., H. Craig, W. B. Broecker, and D. Spencer, *GEOSECS Atlantic, Pacific, and Indian Ocean Expeditions*, vol. 7, *Shorebased Data and Graphics*, 200 pp., National Science Foundation, Washington, D. C., 1987.

Poisson, A., B. Schauer, and C. Brunet, Les rapports des campagnes à la mer à bord du "Marion Dufresne": MD 43/ INDIGO 1, 267 pp., Mission de Recherche, Terres Australes et Antarctiques Françaises, Paris, 1988.

Poisson, A., B. Schauer, and C. Brunet, Les rapports des campagnes à la mer à bord du "Marion Dufresne": MD 49/ INDIGO 2, *Publ. 86-02*, 234 pp., Mission de Recherche, Terres Australes et Antarctiques Françaises, Paris, 1989.

Poisson, A., B. Schauer, and C. Brunet, Les rapports des campagnes à la mer à bord du "Marion Dufresne": MD 55/ INDIGO 3, *Publ. 87-02*, 318 pp., Mission de Recherche, Terres Australes et Antarctiques Françaises, Paris, 1990.

Ponte, R. M., and J. Luyten, Deep velocity measurements in the western equatorial Indian Ocean, *J. Phys. Oceanogr.*, *20*, 44–52, 1990.

Quadfasel, D. R., and F. Schott, Water-mass distributions at intermediate layers off the Somali coast during the onset of the southwest monsoon, 1979, *J. Phys. Oceanogr.*, *12*, 1358–1372, 1982.

Schlosser, P., E. Suess, R. Bayer, and M. Rhein, ^{3}He in the Bransfield Strait waters: Indication for local injection from back-arc rifting, *Deep Sea Res.*, *35*, 1919–1935, 1988.

Schott, F., Seasonal variation of cross-equatorial flow in the Somali Current, *J. Geophys. Res.*, *91*, 10,581–10,584, 1986.

Schott, F., J. C. Swallow, and M. Fieux, Deep currents underneath the equatorial Somali current, *Deep Sea Res.*, *36*, 1191–1199, 1989.

Warner, M. J., Chlorofluoromethanes F-11 and F-12: Their solubilities in water and seawater and study of their distribution in the south Atlantic and north Pacific oceans, Ph.D. thesis, Univ. of Calif., San Diego, 1988.

Warren, B. A., Transindian hydrographic section at lat. 18°S, Property distributions and circulation in the south Indian Ocean, *Deep Sea Res.*, *28*, 759–788, 1981.

Warren, B. A., The deep water of the central Indian Ocean, *J. Mar. Res.*, *40*, suppl., 823–860, 1982.

Wyrtki, K., Physical oceanography of the Indian Ocean, in *Ecological Studies*, vol. 3, *Analysis and Synthesis*, edited by B. Zeitzschel, pp. 18–36, Springer-Verlag, New York, 1973.

C. Andrié, L. Mémery, and L. Merlivat, Laboratoire d'Océanographie Dynamique et de Climatologie, Centre National de la Recherche Scientifique, ORSTOM/UPMC, 4 place Jussieu, 75252 Paris Cedex, France.

D. Jamous and P. Jean-Baptiste, Laboratoire de Géochimie Isotopique, DSM, Commissariat à l'Énergie Atomique, SACLAY, 91191 Gif-Sur-Yvette Cedex, France.

(Received May 14, 1989;
revised December 28, 1990;
accepted May 1, 1991.)